JACS
JOURNAL OF THE AMERICAN CHEMICAL SOCIETY
Article
pubs.acs.org/JACS

Traceless Directing Groups in Radical Cascades: From Oligoalkynes to Fused Helicenes without Tethered Initiators

Kamalkishore Pati, Gabriel dos Passos Gomes, Trevor Harris, Audrey Hughes, Hoa Phan, Tanmay Banerjee, Kenneth Hanson, and Igor V. Alabugin*

Department of Chemistry and Biochemistry, Florida State University, Tallahassee, Florida 32306-4390, United States

Supporting Information

ABSTRACT: We report the first example of a traceless directing group in a radical cascade. The chemo- and regioselectivity of the initial attack in skipped oligoalkynes is controlled by propargyl OR moiety. Radical translocations lead to the boomerang return of the radical center to the site of initial attack where it assists the elimination of the directing functionality via β-scission in the last step of the cascade. The Bu_3Sn moiety continues further via facile reactions with electrophiles as well as Stille and Suzuki cross-coupling reactions. This selective radical transformation opens a new approach for the controlled transformation of skipped oligoalkynes into polycyclic ribbons of tunable dimensions.

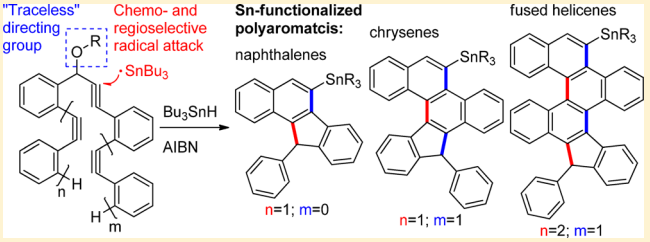

INTRODUCTION

Chemists have a love/hate relationship with protecting and directing groups.[1] Although such groups are very often needed to achieve the desired chemo- and regioselectivity of the key chemical transformation in the presence of multiple targets, but like lingering guests, they remain long after they have overstayed their welcome. However, use of such groups is often unavoidable for achieving sufficient selectivity in cascade transformations of multifunctional reactants.

The problem of selectivity comes to the fore in cascades aimed at the preparation of polyaromatic ribbons from conjugated[2] and skipped[3] oligoalkynes. These processes correspond to controlled "polymerization" of alkyne moieties positioned between the two rows of aromatic rings via a selective sequence of "all-exo" cyclizations.[4] Although the regioselectivity of cyclizations is well controlled by the exopreference for alkyne cyclizations,[5] the key remaining challenge in the design of these cascades involves achieving control over chemoselectivity of initial radical attack. The secondary challenge lies in avoiding the formation of pentagonal units at initiation and termination points of the oligoalkyne cascade. We discuss these challenges below.

For the "polymerization cascade" to proceed to completion by utilizing each of the triple bonds, the initial radical attack should proceed exclusively at the *central alkyne* of the oligoalkyne precursor (Scheme 1).[5a] Such chemoselectivity is difficult to achieve because of the close similarity in the electronic and steric properties of the multiple alkyne units. Initially, we addressed this challenge via covalent attachment of a tethered initiator ("the weak link") which is directed at the correct alkyne target by geometric restraints imposed by the intramolecular trajectory.[5b] Although this approach solves the problem of chemoselectivity of activation, the solution is not ideal because atoms of the tether remain in the molecule after the cascade.

Furthermore, when conjugated oligoalkynes are used as reactants, ring formation from the *first two alkyne moieties* of benzannelated oligoalkynes has to proceed via a 5-exo-dig path (Scheme 2). As a consequence, the "polyacetylene ribbon" formed from the oligoalkyne always contained a pentagonal unit. We have shown that the presence of this pentagon can be avoided when the first reaction between the two alkynes is engineered to follow a 6-exo path, when the starting oligoalkynes are changed from conjugated to "skipped" by adding one extra carbon.

In this work, we disclose a new strategy for chemoselective reactions of oligoalkynes that does not rely on the weak link for radical initiation. Instead, it achieves selective intermolecular attack by using a propargylic methoxy group at the skipped alkynes for directing a tin radical at the correct position where it initiates the full cascade. The use of O-directing functionalities in Sn-radical attack at alkynes has been documented[6] with many interesting examples in the recent work of Hale[7] and Organ.[8]

In order to avoid incorporation of the directing group in the final product, the sequence of bond forming and bond breaking steps in the cascade has to be coordinated to eliminate the directing group *at the last step of the cascade*, with concomitant aromatization of the polycyclic ribbon. Our hypothesis was that the removal of the OMe would benefit from translocation of the radical center if one can design a process where the radical, as a boomerang, returns to the position of the initial intermolecular radical attack to the β-carbon relative to the departing group (Scheme 3).

Under this condition, the loss of directing group occurs via fast β-scission as the last part of a one-pot transformation, and thus, such group can be considered a traceless directing group.[9] Not

Received: October 21, 2014
Published: December 24, 2014

DOI: 10.1021/ja510563d
J. Am. Chem. Soc. 2015, 137, 1165−1180

Scheme 1. Connection between Benzannelated Oligoalkynes and Graphene Ribbons

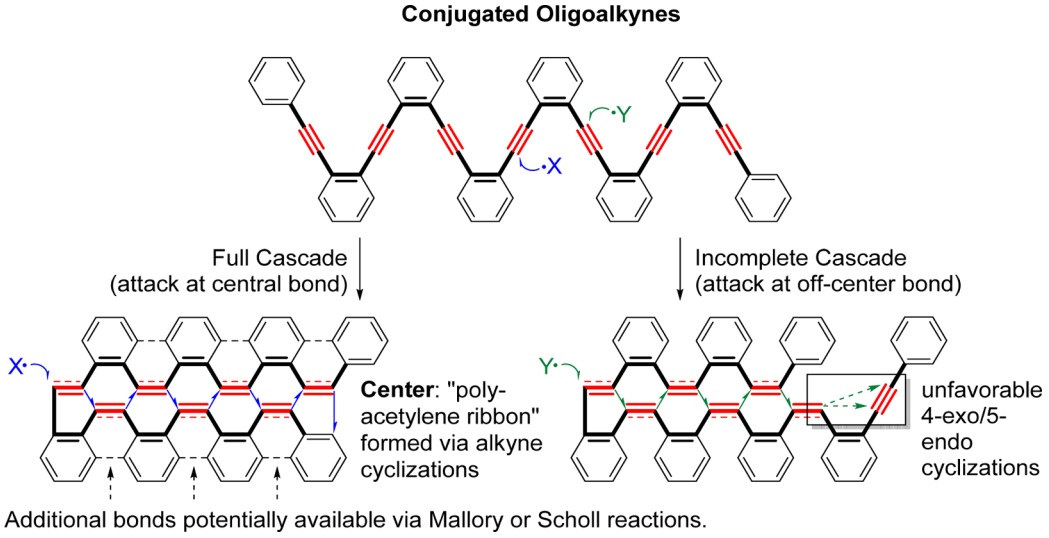

Scheme 2. Evolution of Molecular Design for the Conversion of Oligoalkynes into Polyaromatic Ribbons

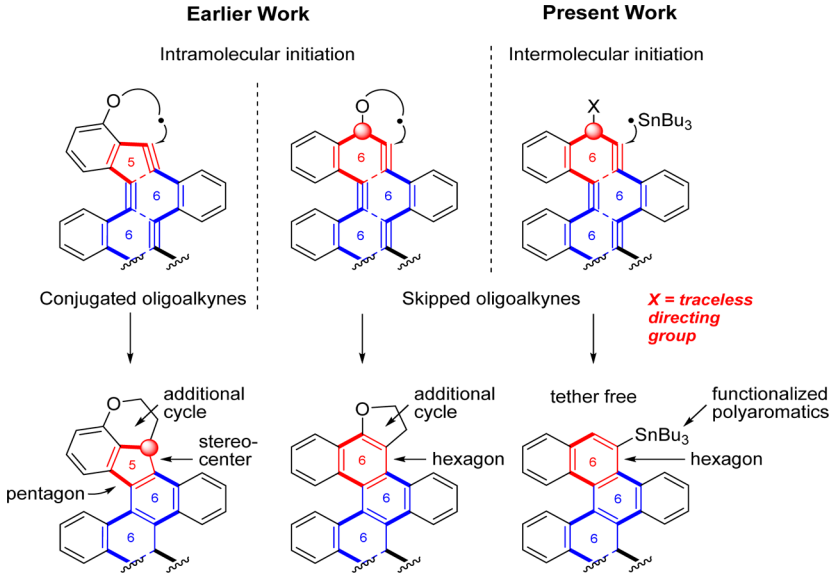

only does this new strategy provide a concise synthetic approach to the defect-free preparation of the top part of the polyaromatic ribbon but also retains the Bu_3Sn substituent as a convenient synthetic handle for further synthetic modifications of the polycyclic framework.

RESULTS

The starting 1,(2-alkynylphenyl)propargyl methyl ethers **1** are readily prepared from commercially available 2-bromobenzaldehydes via a combination of Sonogashira cross-coupling and nucleophilic addition of acetylide anions to the aldehyde (Table 1). The lithiated alkoxide formed at the latter step can be converted either into a propargylic alcohol via protonation or into propargyl methyl ethers via in situ addition of iodomethane. The propargyl methyl ethers **1** were synthesized with a variety of substituents on rings A, B, and C and in good yields (55−90%).

Table 2 shows a screening of various radical reagents and initiators for the model transformation of **1a** to **2a**. The combination of Bu_3SnH and AIBN in refluxing toluene was the most efficient. The failure of silicon reagents indicates that a suitable organotin radical precursor was essential for the success of this cascade. The reaction conditions were further optimized by changing molar ratios of Bu_3SnH/AIBN and varying flow rate using a syringe pump (see Table 3). We found that maintaining a steady concentration of AIBN is preferred over the addition of initiator at once in the beginning of reaction. The addition of 0.04 M Bu_3SnH/0.01 M AIBN mixture at the flow rate of 1 mL/h to the 0.03 M solution of substrate in toluene (110 °C, 14 h) provided **2a** in excellent (86%) yield. Use of lower amounts of Bu_3SnH/AIBN led to incomplete conversions.

The scope of this reaction was verified by the successful cascade cyclization of propargyl methyl ethers shown in Table 4. The range of substituents includes donor and acceptor groups in the core benzene ring as well as at the both alkyne termini. As the result, selective introduction of substituents of varying electronic nature at specific positions of rings A, B, and C (Table 4) of the polycyclic product is possible. Although reaction conditions were not optimized for each of the substrates **2b**−**2r**, the isolated yields remained consistently high for both the donor and the acceptor

DOI: 10.1021/ja510563d
J. Am. Chem. Soc. 2015, 137, 1165−1180

Scheme 3. Translocation of Radical Coupled with Loss of X

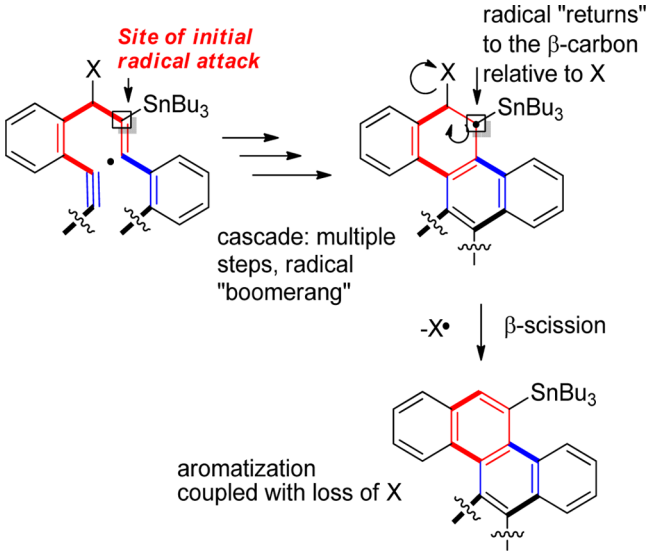

Table 2. Optimization of Reaction Conditions

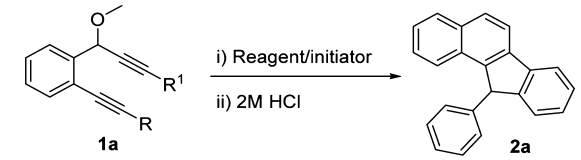

entry	reagent/initiator[a]	condition	yield[b]
1	Bu_3SnH/AIBN	benzene, 16 h, 80 °C	65%
2	Et_3SiH/AIBN	benzene, 16 h, 80 °C	–[c]
3	Et_3SiH/AIBN	toluene, 14 h, 110 °C	–[c]
4	Bu_3SnH/AIBN	toluene, 14 h, 110 °C	86%
5	Ph_3SnH/AIBN	toluene, 14 h, 110 °C	40%
6	Bu_3SnH/ABCN	toluene, 14 h, 100 °C	60%
7	Bu_3SnH/DTBPB	toluene, 14 h, 100 °C	40%
8	Bu_3SnH/Et_3B	THF, 12 h, rt	–[c]
9	Bu_3SnH/Et_3B	benzene, 14 h, 70 °C	–[c]

[a]1.3 equiv of reagent and 0.4 equiv initiator. [b]Isolated yields from silica chromatography. [c]Unreacted starting material (60%, 30%, 65%, and 75%, respectively) and complex mixture of products.

substituents (70–88%), indicating generality and robustness of this cascade transformation.

To examine the role of the methoxy substituent in the radical cascade, two alternate substrates were prepared: a free propargyl

Table 1. 1-(2-Alkynylphenyl)propargyl Methyl Ethers

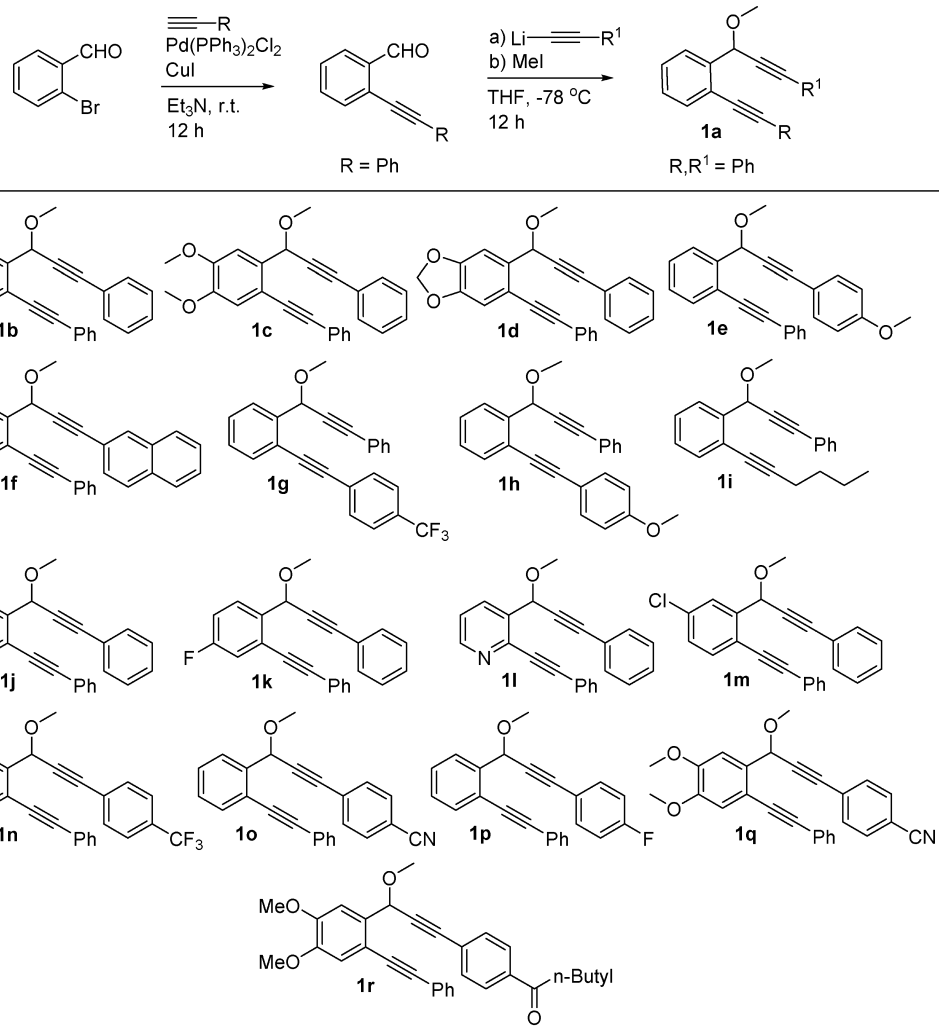

DOI: 10.1021/ja510563d
J. Am. Chem. Soc. 2015, 137, 1165–1180

Table 3. Further Optimization of Bu_3Sn Addition to Alkyne 1a

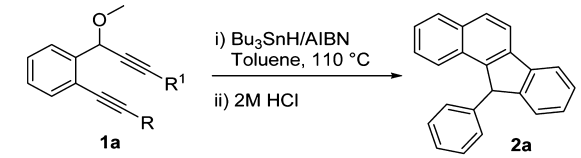

entry	AIBN[a] (equiv)	Bu_3SnH (equiv)	rate	conversion	yield[b]
1	1	1	all at once[c]	60%	40%
2	1	2	all at once	70%	60%
3	1	1.5	AIBN at once, Bu_3SnH 2 mL/h	80%	70%
4	0.5	1.5	Bu_3SnH + AIBN, 2 mL/h[d]	100%	76%
5	0.5	1.5	Bu_3SnH + AIBN, 1 mL/h	100%	86%
6	0.4	1.3	Bu_3SnH + AIBN, 1 mL/h	100%	86%
7	0.2	1.5	Bu_3SnH + AIBN, 1 mL/h	60%	50%

[a]Equivalents are based on proportion to starting material. [b]Isolated yields after column chromatography. [c]Total concentration 0.03M. [d]Condition A: AIBN and Bu_3SnH were dissolved in 2 mL toluene together. Condition B: AIBN and Bu_3SnH were dissolved separately and added simultaneously. Conditions A and B showed no change in yield (all reactions performed under argon atmosphere).

Scheme 4. Control Experiments: Effect of Propargylic Substitution on Selectivity

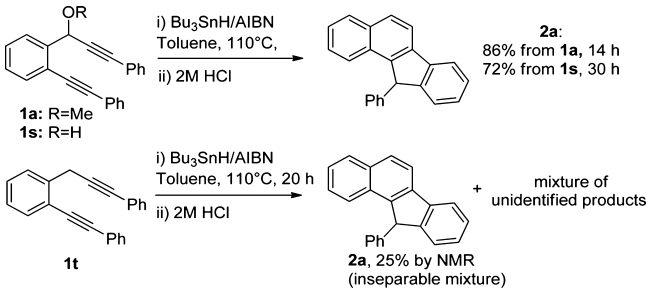

alcohol **1s** and a "deoxygenated" analogue with an unsubstituted methylene bridge **1t** (synthesis of these compounds is described in the Supporting Information (SI)). Even though the reaction of the free alcohol was noticeably slower than the reaction of propargylic ether **1a**, it still displayed comparable level of selectivity, providing an attractive synthetic alternative to the reactions of OMe-substituted substrates. On the other hand, the reaction of the "deoxygenated" substrate **1t** is significantly less selective (Scheme 4). Yields and reaction times for these experiments suggest that the presence of the oxygen substituent plays an important role in the selectivity of this cascade reaction.

Structure Determination. Structures of the products were determined by the combination of ^1H and ^{13}C NMR spectroscopy, which was complemented, in selected cases, by X-ray crystallography.[10] The characteristic ^1H NMR features include disappearance of the reactants' OCH_3 and the propargylic H peaks (at 3.5−3.7 and 5.3−5.9 ppm, respectively) to give rise to a 5.1−5.8 ppm singlet for the remaining sp^3 C−H in the products. In ^{13}C NMR, disappearance of the OCH_3 (56−58 ppm), propargylic CH (71−73 ppm), and the four alkynyl carbons (84−92 ppm) along with the appearance of a signal at 52−55 ppm for the sp^3 carbon in the partially reduced five-membered ring indicated completion of the cascade.

The naphthalene and phenylene moieties in the benzofluorene skeleton of 11-phenyl-11H-benzo[*a*]fluorene **2a** are approximately coplanar suggesting that efficient conjugation and electronic communication should be possible between the different parts of the molecule. On the other hand, the exocyclic aryl group is projected away from the polycyclic plane and oriented in a way that minimizes steric repulsion with the aromatic hydrogens (Figure 1).

Chemo- and regioselectivity of Sn addition was confirmed by X-ray analysis of Sn-precursor of 14-fluoro-11-phenyl-11H-benzo[*a*]fluorene **2p-Sn** (Figure 2). As expected, the Sn atom has approximately tetrahedral geometry with connections to one sp^2 and three sp^3 carbon atoms. Surprisingly, the average of Sn−C_{sp^3} bond lengths (2.163 Å) is smaller than the Sn−C_{sp^2} distance (2.171 Å).[11] The anomalously long bond length in the latter case can be attributed to the steric repulsion between the bulky Bu_3Sn group and ortho-hydrogens of the polyclic moiety. Furthermore, the steric clash of the butyl groups and the polycyclic structure leads to the deviation of C−Sn−C angles (106.93°−114.96°) from the ideal 109.5° tetrahedral valence angle and the slight (~6°) deviation of Sn atom from the benzo[*a*]fluorene plane.

Computational Details. The computational analysis of potential energy profiles involved in this multistep transformation was performed in Gaussian 09[12] with unrestricted M06-2X functional[13] due to its relatively accurate description of reaction and activation energies for a variety of chemical processes including radical reactions.[14] The LanL2DZ basis set was used for Sn. Chemcraft 1.7[15] and CYLView[16] were used to render the molecules and orbitals. Frequency calculations were performed to confirm each stationary point as either a minimum or a first-order saddle point. NBO 3.0 program was used to analyze electronic properties of reactive intermediates.[17]

RESULTS AND DISCUSSION

Chemoselectivity in Radical Cascades. Chemoselectivity is a key challenge in the design of cascade transformations of multifunctional substrates. In a system, where functional groups are similar or almost identical (i.e., oligoalkynes), such challenge is especially formidable. We had shown earlier that a new application of dynamic covalent chemistry toward reversible radical reactions of Sn-radicals and π-systems can be used for the design of surprisingly selective transformation[18] For example, in reactions of aromatic enynes (Scheme 5) where an intermolecular radical attack can lead to the formation of four different benzylic radicals (each capable of two cyclizations), we observed the formation of a single product out of the eight possible cyclic structures. The preferred product is formed from the attack of the most reactive (vinyl) radical at the most reactive (alkene) π-

DOI: 10.1021/ja510563d
J. Am. Chem. Soc. 2015, 137, 1165−1180

Table 4. Radical Cascade of Propargyl Methyl Ethers

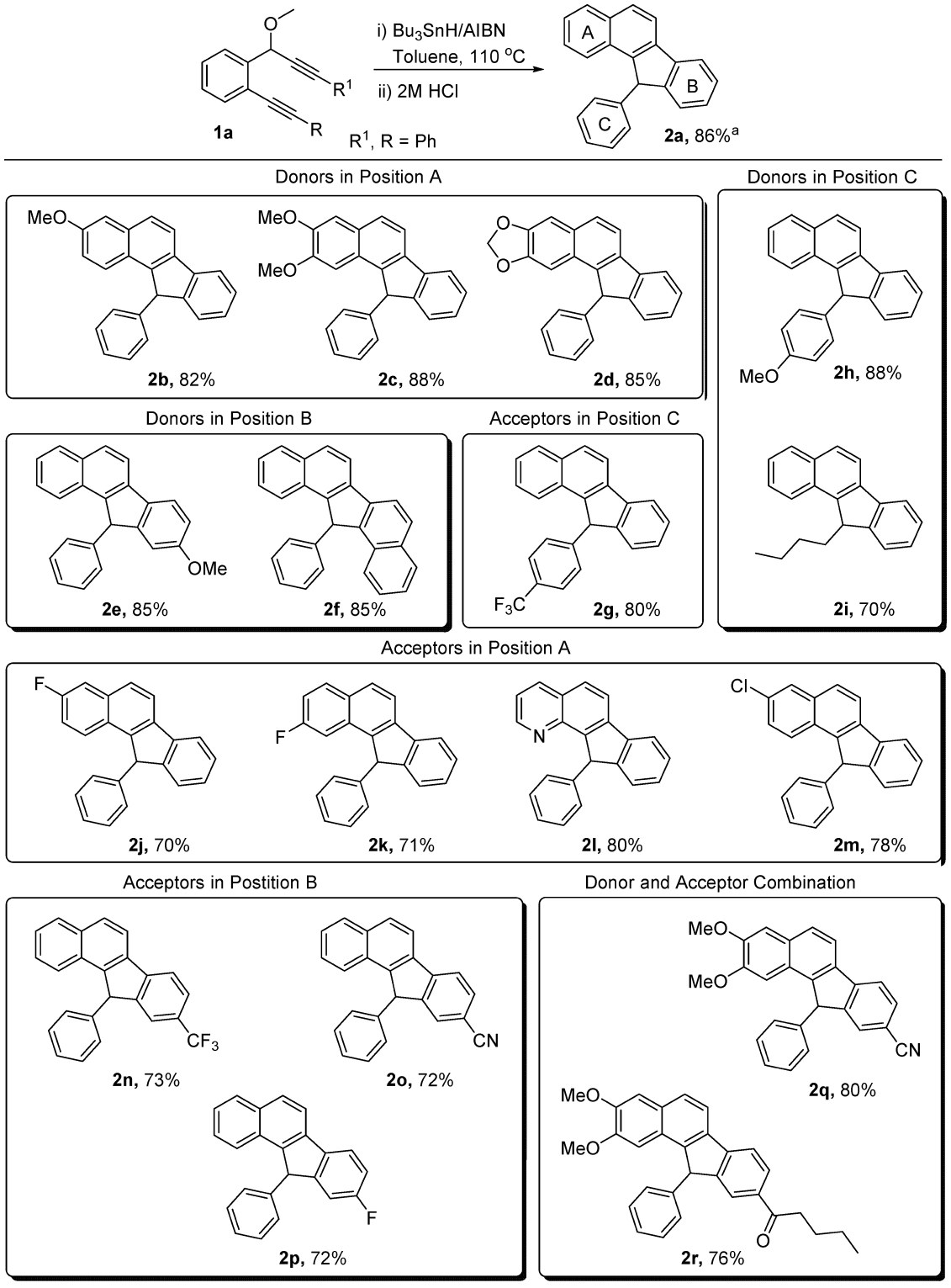

[a]Isolated yields after column chromatography.

bonds via the most stereoelectronically favorable (exo) path. Assuming that the radicals can equilibrate prior to the cyclization, this process can be characterized as a kinetic self-sorting of a pool of the four equilibrating radicals via reaction with the lowest activation barrier. In accord with the Curtin−Hammett principle, under the conditions where addition of Sn radicals is reversible, it is not the relative stability of radicals but the absolute energies of the respective cyclization transition states (TSs) that matter.

The equilibrium between vinyl radicals is supported by the literature reports confirming that addition of vinyl stannanes to double bonds is reversible.[19] For example, Sn radicals are known to isomerize alkenes fast and much faster than Si-based radicals.

DOI: 10.1021/ja510563d
J. Am. Chem. Soc. 2015, 137, 1165−1180

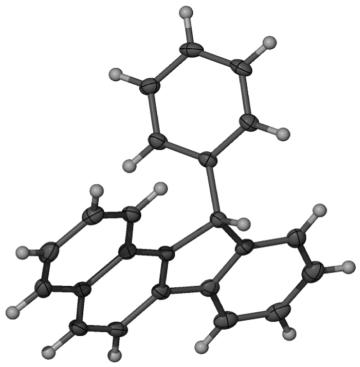

Figure 1. ORTEP diagram for **2a**.

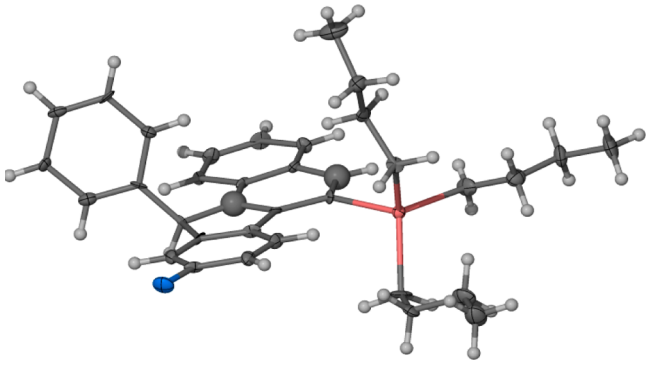

Figure 2. ORTEP diagram for **2p-Sn**.

However, at this point, the "radical pool" is a hypothetical model to fit the observed results.

Alternatively, a simpler source of selectivity can be found in a kinetic preference for the Sn-radical attack at the propargylic position. Such attack would directly provide the correct radical, positioned properly for initiating the cascade. In order to test for applicability of the two models to the present system, we evaluated the relative reactivity of the two types of substituted alkynes separately by carrying out an intermolecular competition experiment between propargyl ether **3** and the diaryl alkyne **4** to determine the relative reactivity of these functionalities toward Bu_3SnH/AIBN system.

Scheme 6 summarizes competition experiments for the 1:1 ratio mixture of propargylic ether **3** and diphenyl acetylene **4** at the previously optimized cyclization conditions. Whereas the propargylic ether was completely consumed, tolane **4** remained unreacted. The simplest rationale for these experimental result is that the presence of the propargylic methoxy substituent directs Sn addition by accelerating kinetic attack at the adjacent alkyne carbon.[20]

Guided by these results, we found that the calculated barrier for $SnMe_3$ radical addition at the propagylic position is remarkably low: $\Delta G^{\ddagger}$ (110 °C) = 4.2 kcal/mol. The relatively low energy of the TS can be rationalized by the several interactions between oxygen lone pairs, the π system, and the Sn radical as illustrated by the NBO energies in Scheme 7. Such transition-state stabilization derives, at least partially, from unusual three-electron interactions between the lone pair of oxygen and the radical orbital at Sn to guide radical attack at the required position.

To better understand the thermodynamic landscape, we also compared the relative stabilities of the four vinyl radicals that can be formed from the skipped diyne **1a** and R_3Sn radical. Furthermore, we had also considered the fifth possibility: formation of a 2c,3e bond between the radical and the oxygen's lone pair, but these species did not correspond to the separate energy minimum and converged to the most stable vinyl radical **A** without barrier. Both ΔE and ΔG (taking the energy of the separated enediyne and the SnR_3 radical as the reference point) were calculated for the four intermediates **A**, **B**, **C**, and **D** (using a truncated, Me_3Sn substituent). In this system, the radical intermediate leading to the experimentally observed pathway was found to be significantly more stable than the other vinyl radicals in Scheme 8. This difference in stability originates from a combination of several factors. First, the two more stable radicals (**A** and **D**) enjoy benzylic stabilization. However, efficiency of benzylic resonance can be attenuated by steric effects. Furthermore, other electronic effects can also offer significant stabilization and complicate the overall situation. For example, the only nonbenzylic radical (**B**) is, somewhat surprisingly, more stable than radical **C**. This inversion of stability may be at least partially derived from the captodative stabilization of the radical center by a vicinal acceptor (C−O) and a vicinal donor (C−Sn) bonds flanking radical **B**.

Figure 3 illustrates the calculated geometries for the four vinyl radicals **A**−**D**. In all four radicals, the vicinal C−Sn bond is aligned with the radical orbital in order to maximize stabilizing hyperconjugative interaction with the radical. Despite a literature suggestion that this interaction is unimportant,[21] NBO analysis find this interaction to the strongest among the interactions of σ_{Sn-C} with the vicinal orbitals. Although this interaction is

Scheme 5. Illustration of the Proposed Radical Pool Concept for the Cyclization of Conjugated Enynes[18a]

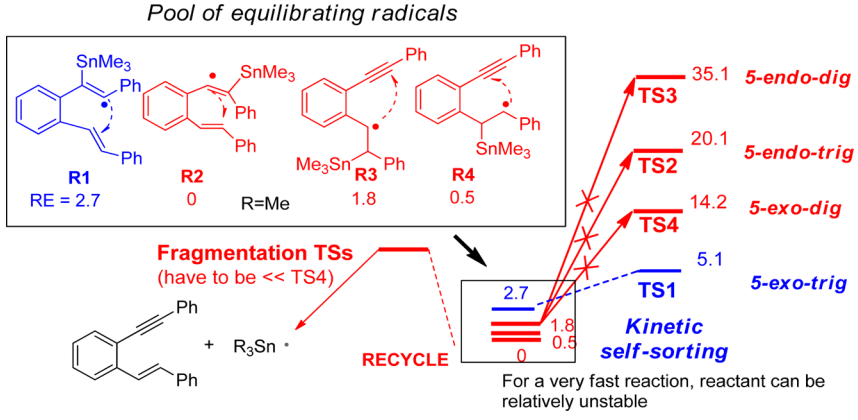

DOI: 10.1021/ja510563d
J. Am. Chem. Soc. 2015, 137, 1165−1180

Scheme 6. Intermolecular Competition in Radical Hydrostannation of Alkynes: Propargylic Ether 3 vs Diphenyl Acetylene (tolane) 4

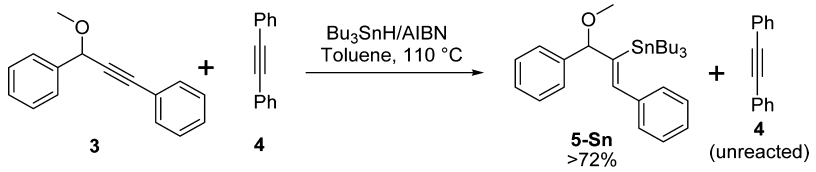

Scheme 7. Selected Electronic Interactions (NBO analysis in kcal/mol) Contributing to the Structure and Stability of the Me_3Sn Radical Addition to the Bis-Alkyne 1a To Form the Most Stable Radical A[a]

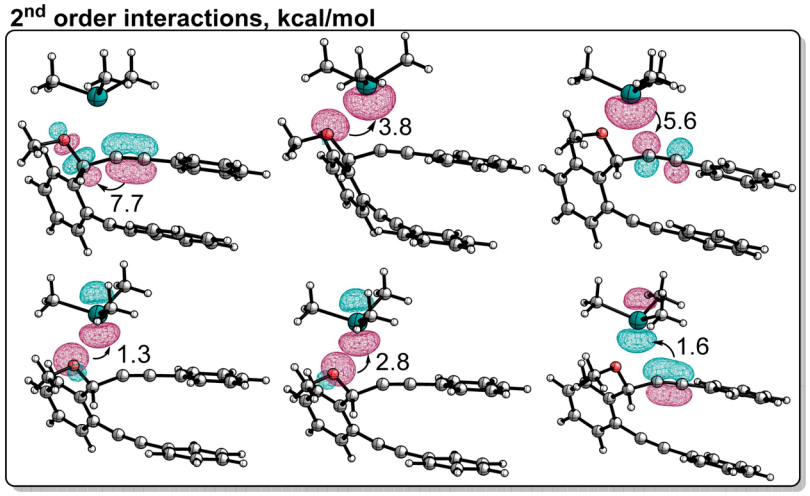

[a]Note that the radical center (n_{Sn}) is half occupied and, unlike a lone pair, can serve as either a donor or an acceptor in second-order delocalizing interactions. Top left: (α- and β-spins summed) $\pi_{C-C} \rightarrow \sigma^*_{C-O}$; top center: ($\alpha$-spin) $sp^{1.12}$ $n_O \rightarrow n_{Sn}$; top right: (α-spin) $n^*_{Sn} \rightarrow \pi^*_{C-C}$. This interaction is responsible for the formation of Sn−C bond. Bottom left: (β-spin) $sp^{3.67}$ $n_O \rightarrow n_{Sn}$; bottom center: (β-spin) $sp^{3.07}$ $n_O \rightarrow n_{Sn}$; Bottom right: (β-spin) $\pi_{C-C} \rightarrow n_{Sn}$.

Scheme 8. Relative Free Energies of the Four Vinyl Radicals Formed by Radical Attack at the Triple Bonds of the Skipped Enediyne 1a at 110 °C

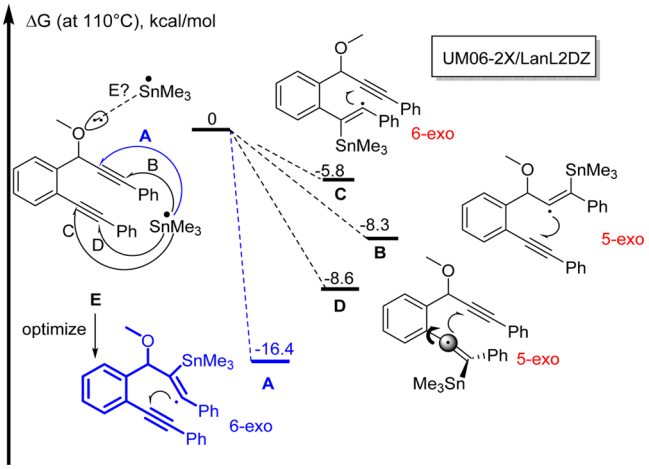

common for all four species and can be neglected in the discussion of their relative stability, it is likely to impose significant effect on the subsequent reactivity for each of the radicals.

Although the most stable radical **A** is the only one where the strong hyperconjugative donor (σ_{C-Sn}) is positioned vicinally to a strong hyperconjugative acceptor (σ^*_{C-O}), the respective $\sigma_{C-Sn} \rightarrow \sigma^*_{C-O}$ interactions is relatively small (3.65 kcal), considerably smaller than interaction of the C−Sn bond with the radical center (26 kcal). The high acceptor ability of radical center in comparison to that of the C−O bond can be explained by the combination of more favorable stereoelectronic arrangement with the lower energy of the acceptor radical orbital. In particular, while the gap between the C−Sn bond is 0.43 au, the gap between C−Sn and σ^*_{C-O} is 0.73 au, as shown at Scheme 9. The efficiency of overlap can be evaluated via the comparison of Fock matrix elements between the donor and acceptor orbitals. Interaction energies can be evaluated via second-order perturbative approach as $\Delta E^{(2)}_{ij} = q_i|F_{ij}|^2/(\varepsilon_j^{(NL)} - \varepsilon_i^{(L)})$. In this case, the F_{ij} term for C−Sn bond and radical center is 0.143 au, whereas the same term for $\sigma_{C-Sn} \rightarrow \sigma^*_{C-O}$ is ~0.046 au. Interestingly, the NBO analysis also finds a remote through-space $n_O \rightarrow \sigma^*_{Sn-C}$ interaction (2.5 kcal) between propargylic oxygen and Me_3Sn moiety. The other vinyl radicals showed slightly different combinations of similar interactions, suggesting that the overall energies result from a complex interplay between numerous electronic and steric effects (Scheme 9).

Barriers for the Cyclizations of Vinyl Radicals. We also calculated the barriers for potentially important cyclizations for the three stable radicals: the most stable radical that can do a 6-exo-dig ring closure and the less stable radicals that can do the potentially faster 5-exo-dig cyclizations. All values are for ΔG in kcal/mol at 110 °C (the experimental temperature).

The 13.8 kcal/mol barrier for 6-exo-dig cyclization of the most stable radical **A** suggests that this reaction will provide the lowest energy path for the escape from the pool, when the next most stable radical **D** has the barrier for its fastest cyclization that

DOI: 10.1021/ja510563d
J. Am. Chem. Soc. 2015, 137, 1165−1180

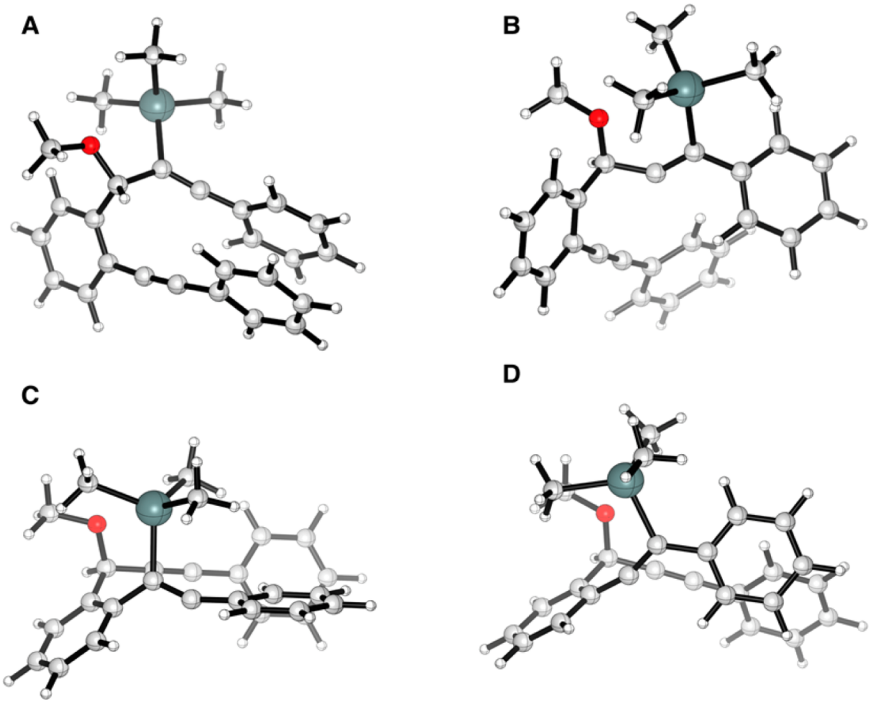

Figure 3. Calculated geometries of the four vinyl radicals **A**–**D** at UM06-2X/LanL2DZ level of theory.

Scheme 9. Selected Electronic Interactions (NBO Energies in kcal/mol) Contributing to the Structure and Stability of Three Vinyl Radicals A, C, and D[a]

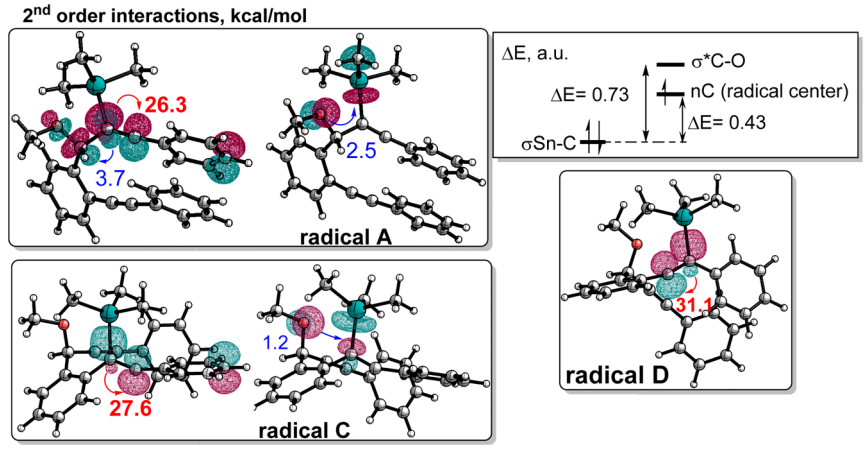

[a]Top left: $\sigma_{Sn-C} \rightarrow$ radical, $\sigma_{Sn-C} \rightarrow \sigma^*_{C-O}$, and $n_O \rightarrow \sigma^*_{Sn-C}$ interactions for radical **A**. Top right: Rationale for the greater acceptor ability of radical center in comparison to σ^*C−O orbital based on contrasting energy gaps between these two acceptor orbitals and the donor σ_{Sn-C} orbital. Differences in the overlap (not shown) play an additional role. Bottom left: $\sigma_{Sn-C} \rightarrow$ radical and $n_O \rightarrow \sigma^*_{Sn-C}$ interactions for radical **C**. Bottom right: $\sigma_{Sn-C} \rightarrow$ radical and $n_O \rightarrow \sigma^*_{Sn-C}$ (not shown for clarity, 0.7 kcal/mol) interactions for radical **D**.

substantially exceeds 6.0 kcal (=13.8−7.8, Figure 4). The cyclization is highly exothermic, exergonic and effectively irreversible.

Indeed, although the 11.8 kcal energy barrier for the 5-exo-dig cyclization of radical **D** is lower than the 6-exo barrier for radical **A** if the respective radicals are taken as the reference points, the *absolute* energy of the 6-exo-dig barrier is lower. This 5-exo barrier is higher than a typical 5-exo-dig barrier[22] due to a stereoelectronic penalty that the reacting radical has to pay for rotating out of conjugation with the central benzene ring in order to attack the triple bond in the TS, as seen in Figure 5.[23]

Such penalty is unique for this radical because, unlike radicals **A** and **C**, radical **D** is conjugated with an aromatic system that is *annealed* to the forming ring. Due to this structural constraint, the central aromatic system is incapable of the same facile rotation that terminal aryl groups in radical **A** and **C** can do without penalty. Since such rotation can result in a ∼10 kcal penalty,[22] this loss of conjugation of radical center with the vicinal phenyl group should account for this relatively high barrier.

Because the above 5-exo-dig cyclization is unusually slow, we also analyzed 5-exo-dig cyclization of radical **B** which does not have to pay the same penalty in the cyclization TS. However, the barrier is only slightly lower (11.3 kcal), presumably due to steric interaction in the TS (Figure 6).

Overall, the calculated energies for the competing radical reactions of the key components of the radical pool can also

DOI: 10.1021/ja510563d
J. Am. Chem. Soc. 2015, 137, 1165−1180

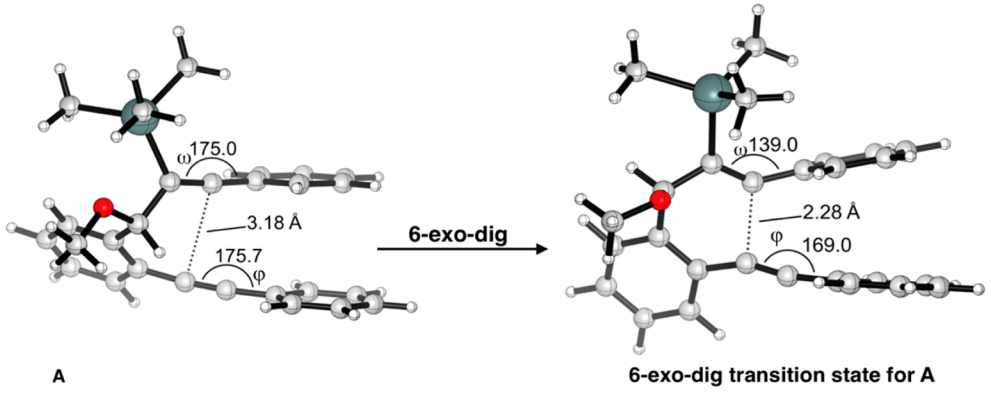

Figure 4. Geometries of radical **A** and its TS for the 6-exo-dig cyclization.

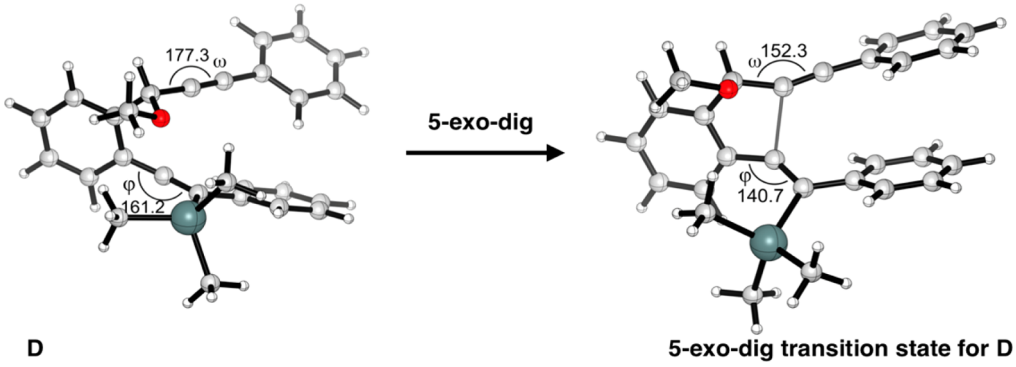

Figure 5. Geometries of the radical **D** and its TS for the 5-exo-dig cyclization.

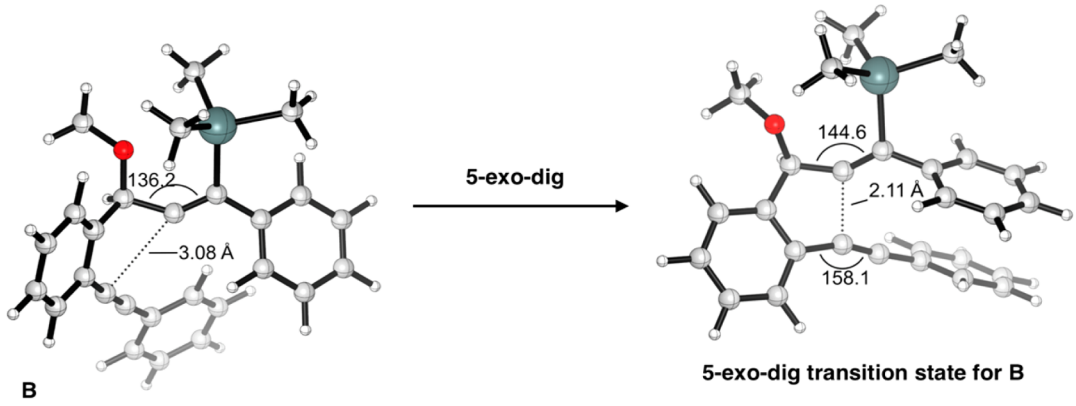

Figure 6. Geometries of the radical **B** and its TS for the 5-exo-dig cyclization.

Scheme 10. Comparison of Relative Energies of the Four Vinyl Radicals and Barriers for Their exo-dig Cyclizations

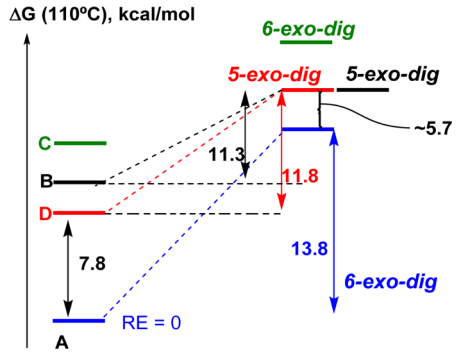

rationalize the observed selectivity of the radical cascade as long as the barriers for radical equilibration are sufficiently low. Note that the present situation is different from that in the radical pool presented in Scheme 5 because the desired 6-exo-dig cyclization will have to compete with two 5-exo cyclizations. As we discussed above, 5-exo-dig barriers are generally lower than the 6-exo-dig alternatives.[12,13] Consequently, in order to achieve selective reaction in this scenario one has either to stabilize the reactant that has to undergo the usually slower 6-exopath to the extent where its cyclization has the lowest absolute energy out of the all possible barriers or destabilize the 5-exo TS for the less stable radicals. The above-discussed stereoelectronic penalty for the unusually slow 5-exo-dig cyclization of radical **D** leads to ~5.7 kcal/mol preference for the 6-exo-dig cyclization of radical **A** (Scheme 10).

DOI: 10.1021/ja510563d
J. Am. Chem. Soc. 2015, 137, 1165−1180

Scheme 11. Proposed Mechanism of Cascade Cyclization[a]

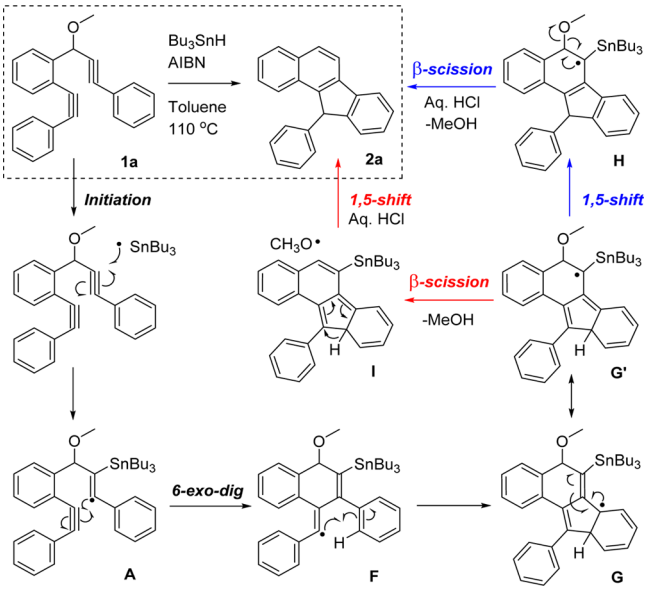

[a]Note the continuous translocation of the radical center through the molecule and conversion of σ-radicals (**A** and **F**) to delocalized π-radicals **G** and **H** where the radical is positioned next to the departing directing group. Color coding for the last two steps corresponds to the color coding in the potential energy surface in Scheme 12.

At the present time, we do not have the sufficiently accurate information about the barriers for C−Sn bond fragmentation in the vinyl radicals **A**−**D** and the barriers for the interconversion in these radicals via metallotropic shifts. In order for the radical pool concept to operate, such barriers have to be lower than the absolute barrier for the 6-exo-dig cyclization of radical **A**. Based on the kinetic preference for the formation of radical **A** (Scheme 6) and the Occam's razor, we rationalize the observed selectivities as a direct facilitating effect of the OR group on the Bu_3Sn attack at the propargylic position followed by trapping of the kinetically formed vinyl radical by a fast and irreversible 6-exo cyclization.

Full Radical Cascade and Return of the Radical at the β-Carbon. The selective 6-exo-dig cyclization discussed in the previous section initiates the experimentally observed cascade. Scheme 11 shows a proposed mechanism involving an initial formation of a radical intermediate **A** formed via the attack of the Bu_3Sn radical at the central alkyne. The subsequent 6-exo-dig cyclization forms the second vinyl radical intermediate **F**. Attack of the neighboring phenyl π-system results in a delocalized radical **G**, leading to rearomatization via a 1,5-hydrogen shift.[24] Finally, fragmentation of intermediate **H** allows for the aromatization of the top ring into a naphthalene moiety. This explanation supports the journey of the radical in this system: it begins with the Bu_3Sn radical attacking the alkyne position vicinal to the directing group starting a boomerang-like radical journey. The vinyl radical is formed, leading to the 5-exo-dig cyclization: this is the furthest position of the radical from where it started. The formation of the 5-membered ring makes the radical closer to its origins but not enough: another resonance structure can be written. At this point the boomerang is back to its initial position, vicinally to the directing and now leaving group. This position is especially interesting because it will end forming a new π bond and making the directing OR group leave the system. *Most importantly, the last step removes the directing group from the product, making this directing approach traceless.* The other approach is that **G′** can undergo the β-scission of the OR first and then do the 1,5-shift to rearomatize the system. Both possibilities are presented in Schemes 11 and 12.

The proposed reaction mechanism is supported by the calculated free energy profile for the full cascade transformation (Scheme 12). As discussed above, the initial 6-exo-dig cyclization is moderately fast but highly exergonic and effectively irreversible. Subsequent attack at the aromatic ring proceeds via a slightly higher (15.2 kcal) barrier. This process is mildly exergonic and moves system even down the potential energy path. As a consequence, even the relatively high barrier for the subsequent 1,5-hydrogen shift (18.6 kcal) is still lower in the *absolute* energy than the two previous barriers, so the cascade can move forward. Because the 1,5-shift leads to aromatization, it is highly exergonic and takes the system ~62 kcal lower than the original vinyl radical **A**. The key final β-scission of the directing OR group has a barrier of only 10 kcal for R = Me (a slightly higher 15.4 kcal barrier was calculated for R = H, where reaction was found to proceed slower experimentally). This process is exergonic by ~5 kcal/mol. Furthermore, the released OR radicals can be quickly intercepted via other thermodynamically favorable processes (e.g., H-abstraction from Bu_3Sn−H, propagating the cascade).

We had also calculated the alternative pathway where fragmentation precedes 1,5-shift. Overall, the highest barrier on this path is only marginally higher. Considering the challenges in accurate computing of reaction barriers for large Sn-containing species, this path may serve as an alternative to the mechanism outlined above. Interestingly, the barriers for the same reactions are lower when they terminate the cascade in comparison to the analogous barriers when these reactions serve as penultimate step (18.6 vs 7.3 kcal for the 1,5-shift, 10.0 vs 20.6 kcal for the fragmentation). This is a direct evidence for thermodynamic contribution to reaction barrier as outlined by the Marcus theory.[24] When the two reactions terminate the cascade, they are assisted by significant aromatic stabilization (formation of one aromatic ring for fragmentation and two aromatic rings for 1,5-shift).

An interesting stereoelectronic feature is observed in the computed fragmentation TS where steric repulsion between the bulky Me_3Sn moiety and the OMe group helps in pushing the OMe group away from planarity and aligning breaking C−O bond with the aromatic π-system. This effect, which can be classified as steric assistance, should be increased further in the real system which has an even more bulky Bu_3Sn moiety instead of the Me_3Sn group used in the computational analysis. If these expectations are correct, the experimental fragmentation barrier should be lowered even further.

Possible Involvement of Cationic Intermediates. An altnernative explanation to the directing effect of the propagylic OR group on the regioselective addition of Sn-radicals to alkynes was made by Organ and co-workers who, on the basis of a careful experimental study, suggested the involvement of Bu_3Sn cations in the selectivity-determining step.[7a] This applicability of this scenario to our system is further discussed and analyzed computationally in the SI. In short, our results suggest that cationic pathway is unlikely to be involved in our radical cascade.

Functionalization of Stannyl Benzofluorenes. Two practical conclusions can be obtained from these results. First, this cascade provides a practical synthetic approach to substituted benzo[*a*]fluorenes, the class of compounds with known anticancer activity.[25] Furthermore, the Sn-containing products can be introduced in reactions with a variety of electrophiles. For example, they can be readily protodestannylated to yield the

DOI: 10.1021/ja510563d
J. Am. Chem. Soc. 2015, 137, 1165−1180

Scheme 12. Calculated Energy Profile for the Cascade Radical Transformation of Diyne 1a[a]

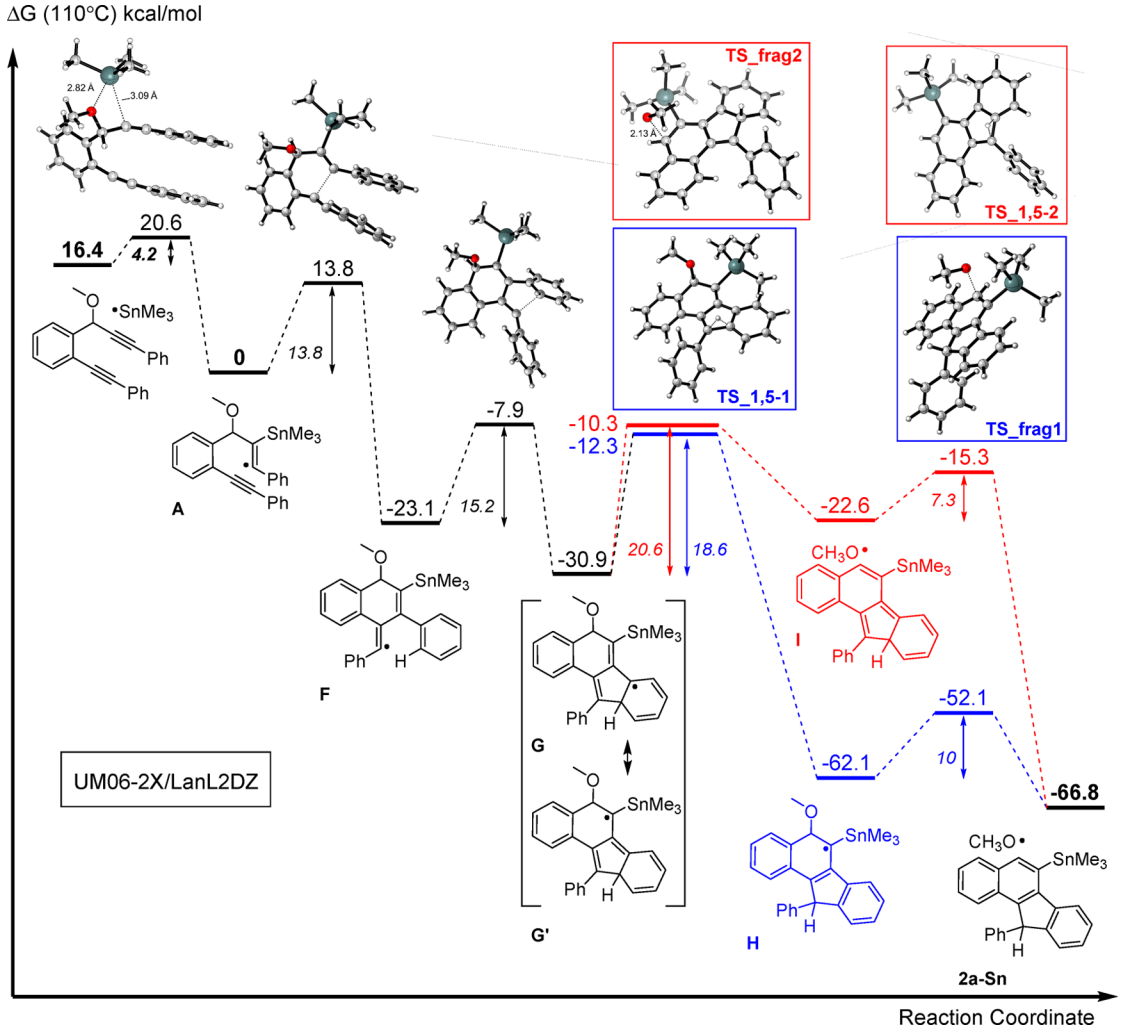

[a]All energies are given relative to radical **A** except for the smaller numbers in italics that correspond to the activation barrier heights relative to the preceding energy minima.

Scheme 13. Derivatization of Benzofluorenes Using Stille and Suzuki Coupling Reactions

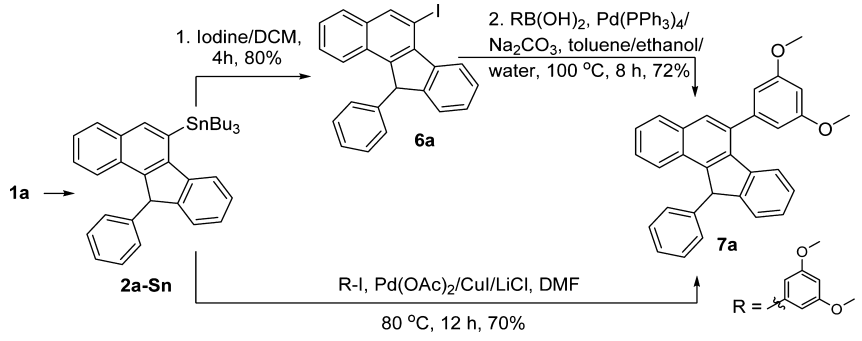

respective hydrocarbon and introduced in Stille cross-coupling. Alternatively, they can be converted into an electrophilic benzofluorenone building blocks via reaction with iodine and/or reacted with carbon nucleophiles, i.e., boronic acids under Suzuki conditions (Scheme 13).[26]

Additionally, the presence of an activating β-OR group in **2b** can be used to direct oxidative dimerization into an expanded polyaromatic system (Scheme 14).

Formation of Larger Polyaromatic Systems. To our satisfaction, the traceless directing group method works very well with the larger oligoalkyne systems. The analogous cascade with a triyne proceeded as planned and provided good yield of a new expanded polyaromatic system. The success of the expanded cascade is consistent with the higher rate of the 6-exo-dig attack at the last triple bond relative to attack of the same vinyl radical at the aromatics.[27] Termination of the cascade with the elimination of the directing OMe group proceeds in exactly the same way as it

DOI: 10.1021/ja510563d
J. Am. Chem. Soc. 2015, 137, 1165−1180

Scheme 14. Oxidative Dimerization of 2b

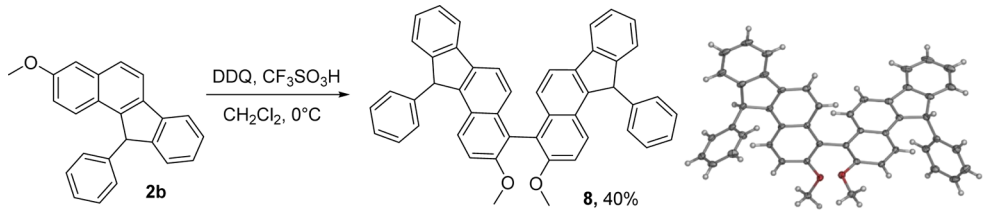

Scheme 15. Cascade Transformation of Skipped Tris-Alkyne 1u and X-ray Geometry of the Product

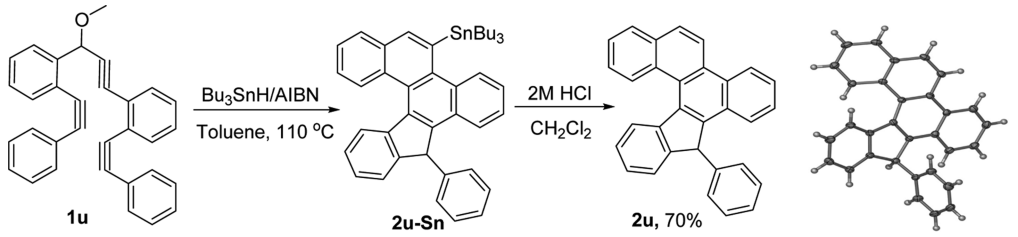

Scheme 16. Cascade transformation of skipped tetraynes 1v–x leads to the formation of diastereomeric helicenes

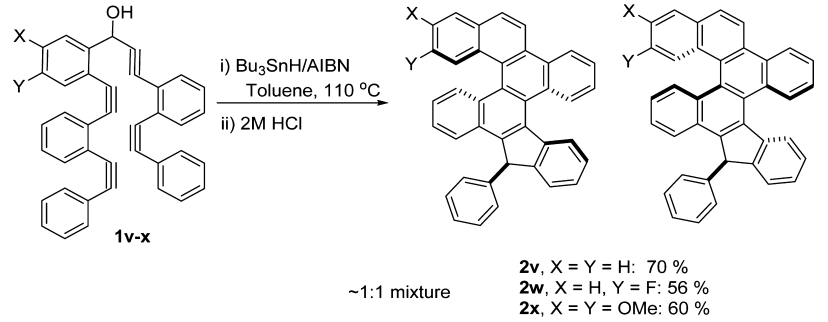

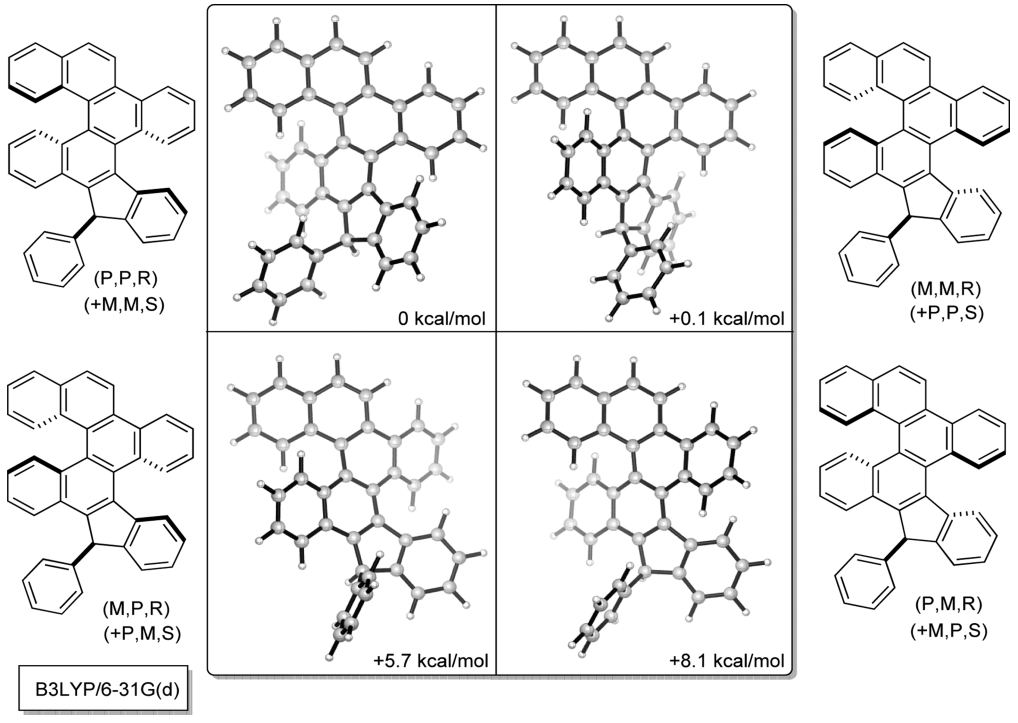

Figure 7. Geometries and energies of the four diastereomeric fused helicenes **2v** (only one of the two enantiomers is shown for each structure).

does for the formation of benzofluorenes in the previous section (Scheme 15).

Addition of the forth alkyne moiety to the reactants introduced the new level of structural complexity in the cascade products.

DOI: 10.1021/ja510563d
J. Am. Chem. Soc. 2015, 137, 1165–1180

Table 5. Photophysical Properties of Select Complexes in CH_2Cl_2

		emission at rt				
complex	absorbance λ (nm)	λ_{max} (nm)	τ (ns)	Φ_{PL}	k_r ($\times 10^7$ s^{-1})[a]	k_{nr} ($\times 10^8$ s^{-1})[b]
2a	257, 266, 316, 344	365, 384	1.5	0.091	6.07	6.06
2b	258, 267, 343, 358	372	7.6	0.201	2.63	1.05
2c	258, 268, 319, 337	361, 379	4.3	0.072	1.69	2.18
2m	264, 273, 333, 350	361, 373	6.3	0.165	2.62	1.33
2o	268, 277, 320, 350	357, 373	5.8	0.589	10.23	0.71
2q	276, 284, 329, 344	386	2.9	0.603	20.79	1.37
2u	281, 294, 350, 391	393, 413	11.5	0.193	1.68	0.70
8	266, 276, 326, 370	375, 391	5.9	0.251	4.26	1.27

[a] $k_r = \Phi/\tau$. [b] $k_{nr} = (1\text{-}\Phi)/\tau$.

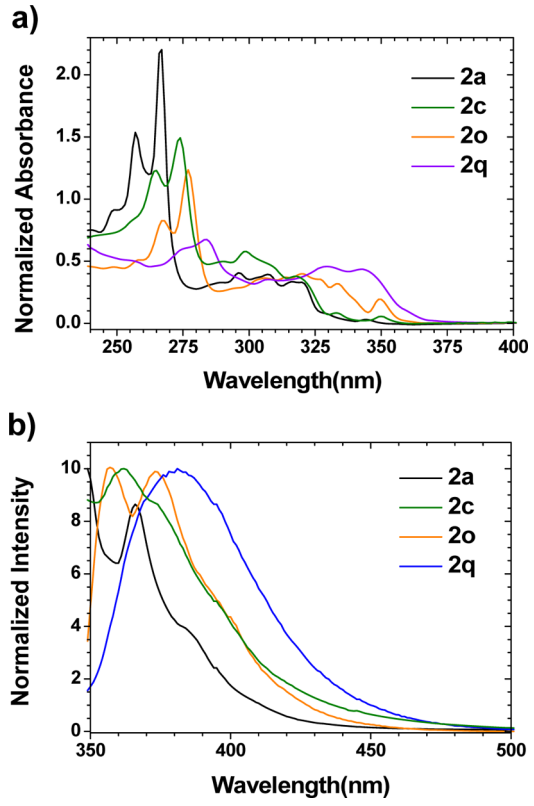

Figure 8. Normalized (a) absorption and (b) emission spectra of **2a**, **2c**, **2o**, and **2q** in CH_2Cl_2 at room temperature. The absorption spectra have been normalized with respect to absorption at 316 nm.

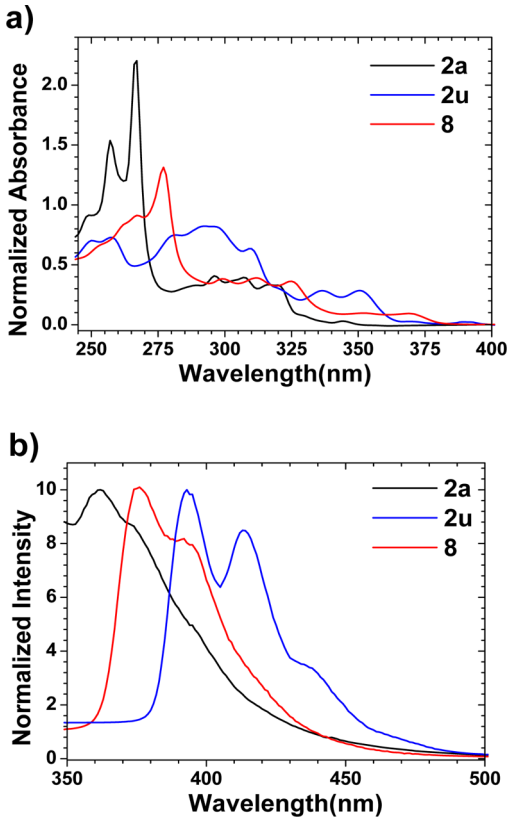

Figure 9. Normalized (a) absorption and (b) emission spectra of **2a**, **2u**, and **8** in CH_2Cl_2 at room temperature. The absorption spectra have been normalized with respect to absorption at 316 nm.

The combination of ^{1}H and ^{13}C NMR data confirmed that reaction still proceeded as above providing fully aromatized products with the loss of OMe moiety and benzofluorene terminus. However, the product was formed as a mixture of two products. All NMR features of these products clearly correspond to the fully complete cascade. We attribute this observation to the presence of two diastereomers originating from the formation of chiral center and atropoisomerism of the two spatially close naphthalenes in the helicene moiety (Scheme 16).

In order to facilitate separation of the two diastereomeric helicenes, we attached polarizing substituents to the polycyclic framework. The mixture of the two dimethoxy-substituted products can be separated by crystallization of diastereoisomers from CD_3CN (90% purity).

These structures correspond to the fusion of two different [5]helicenes: one made entirely of benzene rings and the other containing a pentagon. In order to understand the relative influence of the two helicene units at each other, we analyzed the relative energies of the four diastereomers of the parent fused helicene **2v** by DFT (Figure 7). The two stable conformations correspond to the same chirality of the two helicenes (either P, P or M, M), so the preferred geometries of the two fused chirality units are strongly coupled. The mismatched isomers are much higher in energy (~5 kcal and ~8 kcal higher). On the other hand, effect of chirality at the auxiliary sp^3 asymmetric carbon in the two stable stereoisomers is minor (~0.1 kcal). These computational results are consistent with the experimental observation of two isomeric products formed in the ~1:1 ratio.[28]

Selected Photophysical Properties of Benzo[*a*]fluorene Chromophores. The photophysical properties for select compounds were recorded in aerated dichloromethane and the results are summarized in Table 5. Representative spectra are shown in Figure 8, and the remaining spectra are available in the

DOI: 10.1021/ja510563d
J. Am. Chem. Soc. 2015, 137, 1165−1180

Scheme 17. Representative Examples of Traceless Directing Groups

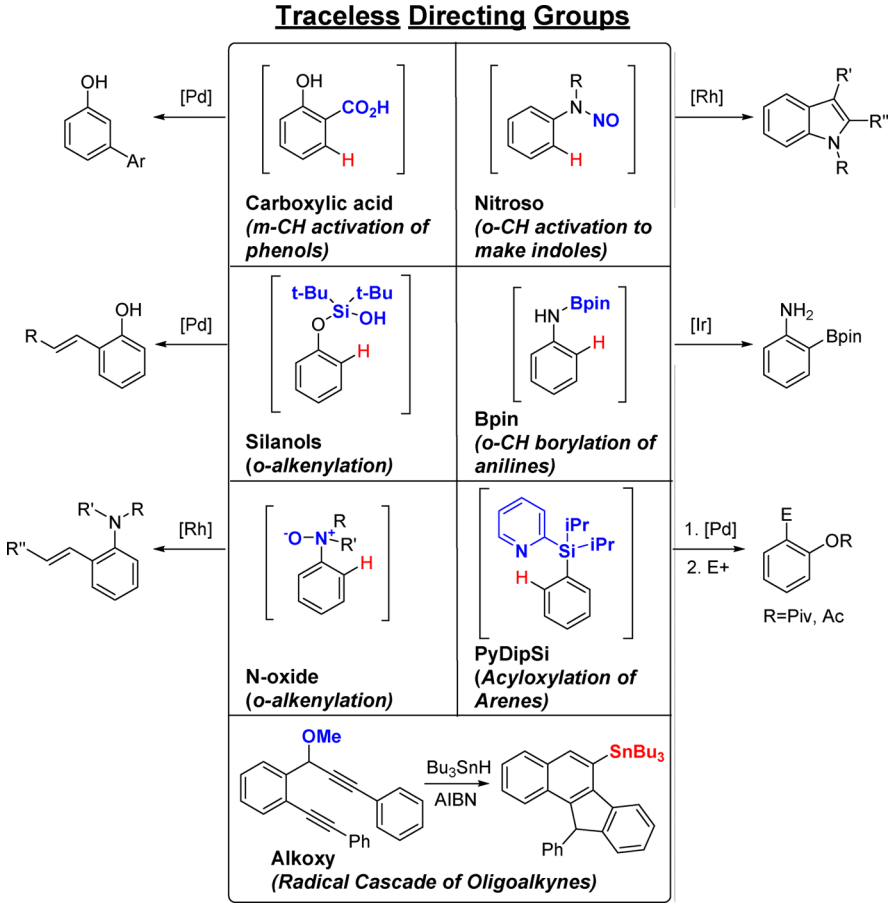

SI. The parent compound, **2a**, exhibits structured absorption features below 350 nm and an emission maximum at 365 nm.

The modular nature of the synthetic method introduced here is ideal for generating multifunctionalized compounds. The energy of absorption and emission peaks are shifted upon substitution. A class of molecules that are of particular interest for their unique photophysical properties are push−pull/donor−acceptor systems, like compound **2q**, which combine electron-withdrawing (−CN) and -donating (-OMe) groups. The relatively unstructured absorption and emission features for **2q** in dichloromethane are indicative of at least some charge-transfer character associated with these transitions. Further support for this assignment is provided by solvent dependent absorption and emission spectroscopy (Figure 8). Compound **2q** exhibits a shift in emission maximum in the order 371, 379, 383, and 399 nm in hexane, 1,4-dioxane, chloroform, and dimethyl sulfoxide, respectively. This bathochromic shift and loss of vibrational features in increasingly polar solvents is attributed to an increase in the molecular dipole moment upon excitation.[29] A similar, albeit less pronounced, bathochromic shift from 326 nm in hexanes to 331 nm in dimethyl sulfoxide is observed in absorption. In contrast, for compound **2a**, which lacks donor and acceptor groups, there is nominal change in both structure and energy (<5 nm) of absorption and emission.

The absorption properties of the compounds are not the only photophysical parameter tunable via substitution. The luminescent quantum yields (Φ) measured at room temperature for the complexes vary between 0.072 and 0.603. The significantly higher quantum yield for **2o** (0.589) and **2q** (0.603), relative to the other complexes (<0.251), is attributed to the significantly higher radiative rate constant (k_r) (Table 5). The enhanced k_r is presumably due to greater excited ground-state coupling. The role of the cyano groups in this increased coupling requires further investigation.

The bathochromic shift observed with **2u** and **8** is due to an increase in the degree of conjugation (Figure 9).

■ CONCLUSIONS

Polycyclic aromatics are important subunits in many natural products, pharmaceuticals, and materials.[30] Alkynes are convenient carbon-rich precursors for the formation of carbon-rich polyaromatics.[31] The advantage of radical cascades[32] stems from their broad functional group tolerance and the combination of high reactivity with controllable selectivity.

In this work, we have developed a new approach for the efficient transformation of skipped oligoalkynes into polycyclic ribbons of tunable dimensions. Incorporation of tin moiety allowed for further functionalization at the initial site of attack via regioselective reactions with electrophiles and Stille and Suzuki cross-coupling reactions. The regioselectivity of the initial attack is directed by propargyl alkoxy moiety which is eliminated at the end of cascade, serving as a traceless directing functionality. Design of complete traceless directing groups is a rapidly developing field with most new designs (i.e., carboxylic acids,[33] silanols,[34] pinacolatoboron(B-pin),[35] and nitroso,[36] *n*-oxide,[37] methyl,[38] PyDipSi,[39] and PyrDipSi,[40] methoxyethyl ether[41] groups) used for catalytic C−H activation as outlined in Scheme 17.

DOI: 10.1021/ja510563d
J. Am. Chem. Soc. 2015, 137, 1165−1180

Examples show above illustrate some of the diversity. Note that in the representative examples shown in Scheme 17, the directing group is *replaced* (sometimes by H, sometimes by a different functionality). Design of radical cascades presented in this work is different because the directing group is not replaced but *eliminated*. Consequently, the present design does not require a separate reaction for the removal of directing group. This step is an integral part of reaction cascade that provides an efficient approach to Sn-functionalized polyaromatics. Furthermore, our work provides a first example of a traceless directing group in a radical cascade.[42]

■ ASSOCIATED CONTENT

Supporting Information

Full experimental details, ^{1}H NMR, ^{13}C NMR, NMR spectra for all of the prepared compounds, X-ray crystallographic data for selected products, and computational details for all calculated structures. Full ref 12. This material is available free of charge via the Internet at http://pubs.acs.org.

■ AUTHOR INFORMATION

Corresponding Author

*alabugin@chem.fsu.edu

Notes

The authors declare no competing financial interest.

■ ACKNOWLEDGMENTS

The fundamental and synthetic aspects of this study were supported by the National Science Foundation (Grants CHE-1152491 and CHE-1213578). We are also grateful to Prof. D. P. Curran (University of Pittsburgh) for valuable suggestions, Dr. B. Gold for helpful mechanistic discussions, a talented group of undergraduate students (D. S. Allenger, C. G. Michas, A. Kavuru, and A. D. Bent) for their assistance in several experiments, and the Research Computing Center of the Florida State University for the allocation of computational resources.

■ REFERENCES

(1) Young, I. S.; Baran, P. S. *Nat. Chem.* **2009**, *1*, 193.

(2) (a) Intermolecular initiation: Alabugin, I. V.; Gilmore, K.; Patil, S.; Manoharan, M.; Kovalenko, S. V.; Clark, R. J.; Ghiviriga, I. *J. Am. Chem. Soc.* **2008**, *130*, 11535. (b) Intramolecular initiation: Byers, P. M.; Alabugin, I. V. *J. Am. Chem. Soc.* **2012**, *134*, 9609.

(3) Pati, K.; Hughes, A. M.; Phan, H.; Alabugin, I. V. *Chem.—Eur. J.* **2014**, *20*, 390.

(4) "All endo-dig" cascades require a different activation mode: Byers, P. M.; Rashid, J. I.; Mohamed, R. K.; Alabugin, I. V. *Org. Lett.* **2012**, *14*, 6032.

(5) General discussion of exoselectivity in radical reactions: (a) Beckwith, A. L. J. *Tetrahedron* **1981**, *37*, 3073. (b) Beckwith, A. L. J.; Schiesser, C. H. *Tetrahedron* **1985**, *41*, 3925. (c) General discussion of selectivity of alkyne cyclizations: Gilmore, K.; Alabugin, I. V. *Chem. Rev.* **2011**, *111*, 6513. (d) Alabugin, I. V.; Gilmore, K.; Manoharan, M. *J. Am. Chem. Soc.* **2011**, *133*, 12608. (e) 5-Exo/6-endo competition in conjugated systems: Alabugin, I. V.; Manoharan, M. *J. Am. Chem. Soc.* **2005**, *127*, 12583.

(6) (a) Konoike, T.; Araki, Y. *Tetrahedron Lett.* **1992**, *33*, 5093. (b) Nativi, C.; Taddei, M. *J. Org. Chem.* **1988**, *53*, 820. (c) Ensley, H. E.; Buescher, R. R.; Lee, K. J. *Org. Chem.* **1982**, *47*, 404. (d) Benechie, M.; Skrydstrup, T.; Khuong-Huu, F. *Tetrahedron Lett.* **1991**, *32*, 7535. (e) Addi, K.; Skrydstrup, T.; Benechie, M.; Khuong-Huu, F. *Tetrahedron Lett.* **1993**, *34*, 6407. (f) Lautens, M.; Huboux, A. H. *Tetrahedron Lett.* **1990**, *31*, 3105. (g) Betzer, J. F.; Delaloge, F.; Muller, B.; Pancrazi, A.; Prunet, J. *J. Org. Chem.* **1997**, *62*, 7768. (h) Willem, R.; Delmotte, A.; De Borger, I.; Biesemans, M.; Gielen, M.; Kayser, F. *J. Organomet. Chem.* **1994**, *480*, 255. (i) Creative applications in total synthesis: Hale, K. J.; Grabski, M.; Manaviazar, S.; Maczka, M. *Org. Lett.* **2014**, *16*, 1164. (j) Micoine, K.; Persich, P.; Llaveria, J.; Lam, M. H.; Maderna, A.; Loganzo, F.; Fürstner, A. *Chem.—Eur. J.* **2013**, *19*, 7370.

(7) (a) Dimopoulos, P.; Athlan, A.; George, J.; Manaviazar, S.; Walters, M.; Lazarides, L.; Aliev, A. E.; Hale, K. J. *Org. Lett.* **2005**, *7*, 5369. (b) Dimopoulos, P.; Athlan, A.; Manaviazar, S.; Hale, K. J. *Org. Lett.* **2005**, *7*, 5373. (c) Dimopoulos, P.; George, J.; Tocher, D. A.; Manaviazar, S.; Hale, K. J. *Org. Lett.* **2005**, *7*, 5377. (d) Manaviazar, S.; Hale, K. J.; LeFranc, A. *Tetrahedron Lett.* **2011**, *52*, 2080.

(8) This group offered an interesting mechanistic explanation of this selectivity based on the transient formation of Sn-cations in a O_2-mediated catalytic cycle: (a) Oderinde, M. S.; Hunter, H. N.; Organ, M. G. *Chem.—Eur. J.* **2012**, *18*, 10817. (b) Oderinde, M. S.; Hunter, H. N.; Froese, R. D. J.; Organ, M. G. *Chem.—Eur. J.* **2012**, *18*, 10821. (c) Oderinde, M. S.; Organ, M. G. *Angew. Chem., Int. Ed.* **2012**, *51*, 9834. (d) Oderinde, M. S.; Organ, M. G. *Chem.—Eur. J.* **2013**, *19*, 2615. (e) Oderinde, M. S.; Froese, R. D. J.; Organ, M. G. *Angew. Chem., Int. Ed.* **2013**, *52*, 11334. (f) Oderinde, M. S.; Froese, R. D. J.; Organ, M. G. *Chem.—Eur. J.* **2014**, *20*, 8579.

(9) Zhang, F.; David, S. *Chem. Soc. Rev.* **2014**, *43*, 6906.

(10) CCDC-1015545 (for **2a**), CCDC-1013214 (for **2p**) and CCDC-1013215 (for **2u**). These data can be obtained free of charge from The Cambridge Crystallographic Data Center via www.ccdc.cam.ac.uk/data_request/cif.

(11) For example, the average bond length of the Sn-C_{sp^2} bonds in triphenyltin 2-pyrimidylthioylacetate is 2.123 Å: Weng Ng, S.; Kumar Das, V. G.; Yip, W. H.; Mak, T. C. W. *J. Chem. Crystal.* **1993**, *23*, 441.

(12) Frisch, M. J. et al. *Gaussian 09*, revision B.01; Gaussian, Inc.: Wallingford, CT, 2009.

(13) (a) Zhao, Y.; Truhlar, D. G. *Theor. Chem. Acc.* **2008**, *120*, 215. (b) Zhao, Y.; Truhlar, D. G. *Acc. Chem. Res.* **2008**, *41*, 157.

(14) Zhao, Y.; Truhlar, D. G. *J. Phys. Chem. A* **2008**, *112*, 1095.

(15) Andrienko, G. A. *ChemCraft*; Bluesnap, Inc.: Waltham, MA, http://www.chemcraftprog.com.

(16) Legault, C. Y. *CYLview*, 1.0b; Université de Sherbrooke: Quebec, Canada, 2009; http://www.cylview.org.

(17) Reed, A. E.; Weinhold, F. *J. Chem. Phys.* **1985**, *83*, 1736. Reed, A. E.; Weinhold, F. *Isr. J. Chem.* **1991**, *31*, 277. Reed, A. E.; Curtiss, L. A.; Weinhold, F. *Chem. Rev.* **1988**, *88*, 899. Weinhold, F. In *Encyclopedia of Computational Chemistry*; Schleyer, P. v. R., Ed.; Wiley: New York, 1998; Vol. *3*, p 1792.

(18) (a) Mondal, S.; Mohamed, R. K.; Manoharan, M.; Phan, H.; Alabugin, I. V. *Org. Lett.* **2013**, *15*, 5650. (b) Mondal, S.; Gold, B.; Mohamed, R. K.; Alabugin, I. V. *Chem.—Eur. J.* **2014**, *20*, 8664. (c) Mondal, S.; Gold, B.; Mohamed, R.; Phan, H.; Alabugin, I. V. *J. Org. Chem.* **2014**, *79*, 7491.

(19) (a) Neumann, W. P.; Albert, H. J.; Kaiser, W. *Tetrahedron Lett.* **1967**, 2041. (b) Kuivila, H. G.; Sommer, R. *J. Am. Chem. Soc.* **1967**, *89*, 5616. (c) Leusink, A. J.; Budding, H. A.; Drenth, W. *J. Organomet. Chem.* **1968**, *11*, 541. (d) Chatgilialoglu, C.; Ballestri, M.; Ferreri, C.; Vecchi, D. *J. Org. Chem.* **1995**, *60*, 3826.

(20) A priori, one can also suggest that the both alkynes undergo fast and reversible Sn-addition, but vinyl radicals produced from the propargylic ether **3** are intercepted via H-abstraction faster.

(21) Dimopoulos, P.; George, J.; Tocher, D. A.; Manaviazar, S.; Hale, K. *J. Org. Lett.* **2005**, *7*, 5377.

(22) Kovalenko, S. V.; Peabody, S.; Manoharan, M.; Clark, R. J.; Alabugin, I. V. *Org. Lett.* **2004**, *6*, 2457. Alabugin, I. V.; Manoharan, M. *J. Am. Chem. Soc.* **2005**, *127*, 12583.

(23) Note also the change from an edge-to-face to the face-to-face interaction between the two terminal Ph groups.

(24) Alabugin, I. V.; Manoharan, M.; Breiner, B.; Lewis, F. *J. Am. Chem. Soc.* **2003**, *125*, 9329.

(25) Jones, C. D.; Blaszczak, L. C.; Goettel, M. E.; Suarez, T.; Crowell, T. A.; Mabry, T. A.; Ruenitz, P. C.; Srivatsan, V. *J. Med. Chem.* **1992**, *35*, 931.

(26) Furthermore, a variety of other functionalization avenues are possible. For example: Ye, Y.; Sanford, M. S. *J. Am. Chem. Soc.* **2013**, *135*,

DOI: 10.1021/ja510563d
J. Am. Chem. Soc. 2015, 137, 1165−1180

4648. Huang, C.; Liang, T.; Harada, S.; Lee, E.; Ritter, T. *J. Am. Chem. Soc.* **2011**, *133*, 13308.
(27) Alabugin, I. V.; Gilmore, K.; Patil, S.; Manoharan, M.; Kovalenko, S.; Clark, R. J.; Ghiviriga, I. *J. Am. Chem. Soc.* **2008**, *130*, 11535.
(28) The pristine [5]helicene has the inversion barrier of ~23 kcal/mol: Janke, R. H.; Haufe, G.; Würthwein, E.-U.; Borkent, J. H. *J. Am. Chem. Soc.* **1996**, *118*, 6031.
(29) Wilde, A. P.; King, K. A.; Watts, R. J. *J. Phys. Chem.* **1991**, *95*, 629.
(30) (a) Georghiou, P. E.; Li, Z.; XAshram, M.; Chowdhury, S.; Mizyed, S.; Tran, A. H.; Al-Saraierh, H.; Miller, D. O. *Synlett* **2005**, 879. (b) Medarde, M.; Maya, A. B. S.; Perez-Melero, C. *J. Enzyme Inhib. Med. Chem.* **2004**, *19*, 521. (c) Sello, G.; Orsini, F. *Mini-Rev. Org. Chem.* **2004**, *1*, 77. (d) Bochkarev, M. N. *Chem. Rev.* **2002**, *102*, 2089. (e) Hoefelmeyer, J. D.; Schulte, M.; Tschinkl, M.; Gabba, F. P. *Coord. Chem. Rev.* **2002**, *235*, 93. (f) For a monograph on the chemistry of naphthalenes and their derivatives, see: Mason, R. T.; Talukder, M.; Kates, C. R. In *Kirk-Othmer Encyclopedia of Chemical Technology*, 4th ed.; Kirk, R. E., Ed.; Wiley, New York, 1995; Vol. *16*, pp 963−1017.
(31) Reviews: (a) Petrukhina, M. A.; Scott, L. T., Eds.; *Fragments of Fullerenes and Carbon Nanotubes: Designed Synthesis, Unusual Reactions, and Coordinate Chemistry*; Wiley: New York, 2011. (b) Chernick, E.; Tykwinski, R. *J. Phys. Org. Chem.* **2013**, *26*, 742. Selected examples: (c) Goldfinger, M. B.; Crawford, K. B.; Swager, T. M. *J. Am. Chem. Soc.* **1997**, *119*, 4578. (d) Feng, X.; Pisula, W.; Müllen, K. *Pure Appl. Chem.* **2009**, *81*, 2203. (e) Scott, L. T.; Jackson, E. A.; Zhang, Q.; Steinberg, B. D.; Bancu, M.; Li, B. *J. Am. Chem. Soc.* **2012**, *134*, 107. (f) Luo, L.; Resch, D.; Wilhelm, C.; Young, C. N.; Halada, G. P.; Gambino, R. J.; Grey, C. P.; Goroff, N. S. *J. Am. Chem. Soc.* **2011**, *133*, 19274.
(32) (a) Curran, D. P. *Synthesis* **1988**, *417*, 489. (b) Jasperse, C. P.; Curran, D. P.; Fevig, T. L. *Chem. Rev.* **1991**, *91*, 1237. (c) Wang, K. K. *Chem. Rev.* **1996**, *96*, 207. (d) Gansauer, A.; Bluhm, H. *Chem. Rev.* **2000**, *100*, 2771. (e) Sibi, M. P.; Manyem, S.; Zimmerman, J. *Chem. Rev.* **2003**, *103*, 3263. (f) Wille, U. *Chem. Rev.* **2013**, *113*, 813.
(33) Luo, J.; Preciado, S.; Larrosa, I. *J. Am. Chem. Soc.* **2014**, *136*, 4109.
(34) Huang, C.; Chattopadhyay, B.; Gevorgyan, V. *J. Am. Chem. Soc.* **2011**, *133*, 12406.
(35) Preshlock, S.; Plattner, D.; Maligres, P.; Krska, S.; Maleczka, R. E., Jr.; Smith, M. R., III. *Angew. Chem., Int. Ed.* **2013**, *52*, 12915.
(36) Wang, C.; Huang, Y. *Org. Lett.* **2013**, *15*, 5294.
(37) Huang, X.; Huang, J.; Du, C.; Zhang, X.; Song, F.; You, J. *Angew. Chem., Int. Ed.* **2013**, *52*, 12970.
(38) Manna, S.; Matcha, K.; Antonchick, A. P. *Angew. Chem., Int. Ed.* **2014**, *53*, 8163.
(39) Chernyak, N.; Dudnik, A.; Huang, C.; Gevorgyan, V. *J. Am. Chem. Soc.* **2010**, *132*, 8270.
(40) Gulevich, A. V.; Melkonyan, F. S.; Sarkar, D.; Gevorgyan, V. *J. Am. Chem. Soc.* **2012**, *134*, 5528. Wang, Y.; Gulevich, A. V.; Gevorgyan, V. *Chem.—Eur. J.* **2013**, *19*, 15836.
(41) Greene, M. A.; Yonova, I. M.; Williams, F. J.; Jarvo, E. R. *Org. Lett.* **2012**, *14*, 4293.
(42) Our definition does not include α-directed reactivity (i.e., modification at the same carbon where directing group is attached) as a recent report of very interesting chemistry that utilizes CO_2H as a "traceless directing group" in radical decarboxylations. Chu, L.; Ohta, C.; Zuo, Z.; MacMillan, D. W. C. *J. Am. Chem. Soc.* **2014**, *136*, 10886. Without this limitation, the list of directing groups would increase dramatically. For example, iodine in atom-transfer reactions of alkyl iodides (i.e., R−I → R• → R−X) or in nucleophilic substitution in alkyl iodides would also be considered a "traceless directing group" in such expanded definition.

DOI: 10.1021/ja510563d
J. Am. Chem. Soc. 2015, 137, 1165−1180